European Journal of Pharmaceutical Sciences 214 (2025) 107250

Contents lists available at ScienceDirect

European Journal of Pharmaceutical Sciences

journal homepage: www.elsevier.com/locate/ejps

pH-stat *versus* pH-shift lipolysis model: Exploring *in vitro-in vivo* relationships for lipid-based formulations of nilotinib

Hannah S. Kirschbaum [a,c], Niklas J. Koehl [b], Johannes A. Blechar [a], Christina Wiesinger [a], Laura J. Koehl [a], Patrick J. ODwyer [c], Martin Kuentz [d], René Holm [e], Christian Jede [a], Brendan T. Griffin [c,*]

[a] Global Analytical Development, Global CMC Development, Merck Healthcare KGaA, Frankfurter Strasse 250, 64293 Darmstadt, Germany
[b] Global Drug Product Development, Global CMC Development, Merck Healthcare KGaA, Frankfurter Strasse 250, 64293 Darmstadt, Germany
[c] School of Pharmacy, University College Cork, Cork, Ireland
[d] Institute for Pharma Technology and Biotechnology, University of Applied Sciences and Arts Northwestern Switzerland, Hofackerstr. 30, Muttenz 4132, Switzerland
[e] Department of Physics, Chemistry and Pharmacy, University of Southern Denmark, Campusvej 55, Odense, Denmark

ARTICLE INFO

Keywords:
In vitro digestion
Lipid-based formulation
pH-stat
pH-shift lipolysis
Supersaturation
In vitro-in vivo relationships (IVIVR)

ABSTRACT

The pH-stat *in vitro* lipolysis method is well established for evaluating lipid-based formulations (LBFs), however the absence of a simulated gastrointestinal transition may lead to an overestimation of drug precipitation particularly in the case of weakly basic drugs. This study aimed to compare the conventional pH-stat method with a pH-shift lipolysis approach by evaluating a diverse set of LBFs using nilotinib, a weakly basic model drug. Additionally, the study sought to assess *in vitro–in vivo* relationships (IVIVRs) and enhance understanding of the predictive capabilities of these models. Four nilotinib-containing LBFs were tested *in vitro*, and pharmacokinetic profiles were evaluated in Sprague Dawley rats. The formulations included a supersaturated Peceol® solution (sLBF), a Peceol® lipid suspension (type I according to the Lipid Formulation Classification System (LFCS)), a type III LFCS medium-chain suspension, and a type IV LFCS suspension. The highest bioavailability was achieved with the Peceol® sLBF and the type III LFCS formulation. Strong IVIVRs were established for both *in vitro* lipolysis models. In conclusion, utilizing both *in vitro* models offered distinct advantages depending on the stage of development and the specific questions being addressed. This approach contributes to more efficient formulation development and a reduced reliance on animal studies in early-stage drug development.

1. Introduction

In drug discovery and development, there is a growing trend towards molecules with increasing molecular weight, hydrophobicity, and/or lipophilicity. These properties may lead to challenges with low aqueous solubility, low permeability, and low oral bioavailability (Holm et al., 2023; O'Driscoll and Griffin, 2008; Stegemann et al., 2023). To address these issues, several formulation strategies have been explored, including solid-based approaches such as amorphous solid dispersions and particle size reduction techniques (Kuentz et al., 2016; Leuner and Dressman, 2000). Among these, lipid-based formulations (LBFs) have emerged as a particularly promising option (Feeney et al., 2016). A key advantage of LBFs over solid-based alternatives is that they are liquid-based solutions, which can facilitate easier dosing in preclinical models and enable more straightforward translation to human studies. LBFs have the potential to improve intestinal solubility and enhance permeability, thereby addressing the absorption and solubility limitations of poorly soluble and poorly permeable drugs (Feeney et al., 2016; Kuentz, 2012; Mu et al., 2013; O'Driscoll and Griffin, 2008). Among the various types of LBFs, Self-Emulsifying Drug Delivery Systems (SEDDS) have gained significant attention. These formulations are isotropic mixtures of oils, surfactants, and co-solvents that spontaneously form fine oil-in-water emulsions upon mild agitation in an aqueous environment, such as the gastrointestinal (GI) tract (Pouton, 2006). LBFs are digested *in vivo* and interact with bile salts and phospholipids, forming colloidal structures that influence the dissolved drug concentration and absorption (Miller et al., 2011; Porter et al., 2007).

In vitro models are commonly used to assess LBF performances by simulating intestinal digestion, particularly the pH-stat lipolysis model is well described and studied (Sek et al., 2002; Zangenberg, 2001), it

* Correspondence author at. School of Pharmacy, University College Cork, Cork, Ireland.
E-mail address: brendan.griffin@ucc.ie (B.T. Griffin).

https://doi.org/10.1016/j.ejps.2025.107250
Received 30 May 2025; Received in revised form 13 August 2025; Accepted 28 August 2025
Available online 29 August 2025

mimics the intestinal digestion in a single compartment set-up. While the pH-stat model provides valuable insights into lipolysis, a key drawback of the model is the lack of an absorptive sink, resulting in drug concentrations that may exceed physiological levels in the intestine (Berthelsen et al., 2019; Stillhart and Kuentz, 2016). This can lead to an increased risk of precipitation during the *in vitro* lipolysis (Griffin et al., 2014; Stillhart et al., 2014). Moreover, the standard pH-stat set-up fails to account for the supersaturation and precipitation that may occur during the transition from the stomach to the small intestine (Huang et al., 2021). This is particularly relevant for weakly basic drugs, which are generally more soluble in the acidic gastric environment and are prone to precipitating when entering the higher pH of the small intestine. Previous studies have reported that it is challenging to establish a robust *in vitro-in vivo* relationship (IVIVR) with the pH-stat model (Berthelsen et al., 2019; Feeney et al., 2016; Huang et al., 2021). The review by Feeney et al. (2016) highlighted that only four out of eight different drugs tested in the pH-stat setup, in at least three LBFs, demonstrated a good correlation. Therefore, there is a need for improved *in vitro* models that can provide more predictive outcomes for LBFs throughout the gastrointestinal process. It is essential to utilize models with an appropriate level of complexity that effectively address specific research questions.

To address the limitations of the pH-stat model, various research teams have created a diverse array of *in vitro* lipolysis models, designed to overcome these limitations with the aim to enhance the predictive power. This is in accordance with the 3R principle (Replacement, Reduction, and Refinement) and has the potential to reduce the reliance on extensive *in vivo* preclinical studies in animals, leading to a more efficient drug formulation evaluation process (Kostewicz et al., 2014). Complexity of these enhanced lipolysis models vary, and the models have been reviewed in detail by Berthelsen et al. (2019). Several models incorporate gastric dissolution and/or a gastric digestion step prior to digestion in the simulated intestinal compartment (Klitgaard et al., 2021; Minekus et al., 2014). The aim of such *in vitro* lipolysis models is to study the precipitation tendency of the drug since one of the main benefits of LBFs is their capacity to maintain the drug solubilisation during the transit. Klitgaard et al. (2020) employed a two-step approach in their digestion model, wherein the simulation began with gastric digestion, and after 30 min, an intestinal medium was introduced into the vessel. With their GI digestion model a consistent rank order of two LBFs *in vivo* and *in vitro* was established. Notably, the rank order was more pronounced with the GI digestion model compared to the pH-stat results.

Most IVIVRs to date have focused on only the lipid classes of the classical Lipid Formulation Classification System (LFCS) types I–IV. This represents a key gap, particularly for challenging compounds like the `brick-dust' molecule nilotinib, a Biopharmaceutical Classification System (BCS) class IV drug with poor solubility in aqueous media and classical LFCS LBF types. Nilotinib is a weak base (pKa of 3.9 and 5.1–5.6) with pH-dependent solubility, poor permeability, high lipophilicity (logP 5.0), and practical insolubility at pH 4.5 and above (FDA, 2023; Koehl et al., 2019; Shukla et al., 2011). As emerging drug candidates increasingly fall outside the scope of traditional LFCS systems, there is a growing need to evaluate alternative LBFs, such as lipid suspensions, supersaturated systems, and nanoemulsions. These may offer distinct advantages in solubility, stability, and bioavailability, and better support the development of effective, translatable drug delivery strategies.

Given the challenges associated with nilotinib's low solubility in lipid vehicles, as described by Koehl et al. (2019), this study investigated four different LBF types containing nilotinib. Three lipid suspensions and a supersaturated LBF solution were employed. Peceol® was selected for a type I LBF due to reported higher solubility in monoglycerides compared to triglycerides (Koehl et al., 2019). Utilizing Peceol®, a supersaturated LBF was prepared. Additionally a surfactant only type IV formulation consisting of a mixture of Tween® 85/Cremophor® RH40 was selected (Koehl et al., 2020c). Based on solubility studies, medium-chain trigylcerides where chosen for the type III formulation, that contains the same surfactants as the type IV, providing a valuable comparison to assess the impact of adding triglycerides to the formulation mixture (Koehl et al., 2019). The study provided new insights by implementing the pH-shift lipolysis model into compendial dissolution testing equipment, facilitating a direct head-to-head comparison with the pH-stat model. Although the pH-stat has been extensively studied, its lack of standardized hydrodynamics remains a limitation. While studies like those conducted by the INFOGEST consortium have highlighted how factors such as reaction vessel volume and shape can influence the extent of digestion (Grundy et al., 2021), further efforts toward standardization are needed. By leveraging existing industry infrastructure, specifically a standard USP-type apparatus, this approach provides more consistent and well-defined hydrodynamic conditions compared to traditional pH-stat systems. With the investigated pH-shift model formulations can be ranked based on their performance during pH-shift and digestion, providing a tool to support formulation decision-making in industrial development. The impact of the simulated digestion on the solubility was analysed and compared with the corresponding *in vivo* pharmacokinetic (PK) data from rats to establish an IVIVR. Finally, the study evaluated whether the increased complexity of the pH-shift model improved the predictive power of IVIVRs compared to the standard pH-stat lipolysis model.

2. Materials and methods

2.1. Chemicals

Nilotinib was obtained from abcr GmbH (Karlsruhe, Germany). The pancreatic extract, Tween® 85 (Polyoxyethylene Sorbitan Trioleate), and Cremophor® RH40 (containing glyceryl polyethylene glycol oxystearate and fatty acid glyceryl polyglyceryl esters) were purchased from Merck KGaA (Darmstadt, Germany). Tricaprin was obtained from Tokyo chemical industry Co (Tokyo, Japan). Peceol® (Mono-, di- and triglycerides of oleic ($C_{18:1}$) acid, the monoester fraction being predominant) was kindly donated from Gattefossè (Saint-Priest, France). 3F powder for the preparation of fasted state simulated intestinal fluid (FaSSIF) was obtained from biorelevant (London, UK). All other chemicals and solvents were of analytical grade or HPLC grade.

2.2. In vitro experiments

2.2.1. Dissolution media

Simulated Gastric Fluid (SGF) was adjusted to pH 2.0 using 1 M HCl in order to minimize the reduction in pH during the intestinal section of the experiment (Jede et al., 2023). The biorelevant medium FaSSIF, that was used for the *in vitro* lipolysis experiments, was prepared using a double-concentrated phosphate buffer at pH 6.5 to maintain the pH of the medium at a constant and physiologically relevant level during pH-shift experiments (Jede et al., 2019). The phosphate buffer contained 77.5 mM NaCl and 56.8 mM of NaH_2PO_4. To prepare the phosphate buffer with a buffer capacity of 10 mmol/L/ΔpH, 106 mM of NaCl and 28.4 mM of NaH_2PO_4 were dissolved and the pH was adjusted to 6.5. To prepare FaSSIF, 1.12 g of 3F powder was added to 500 mL of phosphate buffer, following the preparation guidelines provided by biorelevant.com.

2.2.2. Solubility tests

Solubility of nilotinib in FaSSIF pH 6.5 (10 mmol/L/ΔpH buffer capacity), in FaSSIF pH 6.5 with double-concentrated phosphate buffer with a buffer capacity of 20 mmol/L/ΔpH and in SGF pH 2.0 was assessed using the shake-flask method at 37 ± 5 °C by adding an excess amount of drug substance to 30 mL of preheated media in a 50 mL size flask. The flasks were placed in a water bath at 37 ± 5 °C and shaken. After 24 h, samples were withdrawn and filtered through a 0.2 μm

regenerated cellulose filter, discarding the first 1 mL of the filtrate. The supernatant was then diluted with ACN/water (50:50, v/v) and analyzed with high-performance liquid chromatography (HPLC) as described in Section 2.2.4.

2.2.3. Preparation of the LBFs

The LBFs were prepared similar to the methods outlined by Koehl (2020). The composition of each formulation is shown in Table 1. Briefly, the nilotinib suspensions (10 mg/mL) were prepared by weighing and combining the drug with the lipid excipient and stirring at 37 °C overnight (Koehl et al., 2019). Prior to mixing, Cremophor® RH40 had to be melted at 50 °C and Tricaprin at 37 °C. To prepare the sLBF, nilotinib was weighed into a glass vial and Peceol® was added to achieve a final concentration of 10 mg/mL. The mixture was placed on a heating plate and sealed with parafilm. A continuous nitrogen stream into the vial was installed to prevent oxidation, while the suspension was stirred at 600 rpm, using a magnetic stirring plate. The suspension was heated up to 130 °C and maintained at this temperature for 10 min, followed by cooling to 23 ± 2 °C. Subsequently, two more heating cycles were conducted. The concentration of nilotinib in the formulations was checked via HPLC analysis on the day of lipolysis. A sample was centrifuged at 14,000 rpm and 37 °C for 15 min using a benchtop centrifuge (Centrifuge 5430 R with rotor FA-45–30–11, Eppendorf AG, Hamburg, Germany). The supernatant was diluted sequentially: first in acetonitrile and ethyl acetate (1:3, v/v), then further diluted 1:10 (v/v) in acetonitrile and ethyl acetate (3:1, v/v), finally 1:10 (v/v) in acetonitrile and methanol (35:30, v/v). Samples were measured via HPLC, as described in Section 2.2.4.

2.2.4. In vitro pH-stat lipolysis

The experimental protocol was adapted from Williams et al. (2012b) with an increased overall volume following the protocol of Koehl et al. (2019). In this study a modification of the digestion buffer was made. Instead of using a TRIS maleate buffer for the preparation of FaSSIF, a double-concentrated phosphate buffer with 20 mmol/L/ΔpH buffer capacity at pH 6.5 was utilized. Furthermore, in accordance with recent findings by Ejskjaer et al. (2024), no calcium was added into the digestion media.

The lipolysis was performed using a Titrando® 907 (Metrohm AG, Herisau, Switzerland), comprising an over-head stirrer, a 804 Ti-stand, a pH electrode (Metrohm) and two 800 Dosino® dosing units. The system was operated by the Tiamo® 3.0 software (Metrohm). The composition of the aqueous intestinal media was sodium taurodeoxycholate (3 mM), phosphatidylcholine (0.75 mM), monosodium phosphate (56.8 mM) and NaCl (77.5 mM). The pancreatin extract (USP x 8) was prepared freshly by adding 10 mL of 5 °C blank digestion buffer (phosphate buffer without phospholipids and bile salts) to 2 g of porcine pancreatic enzymes in a 50 mL falcon tube, which was vortexed thoroughly. The mixture was centrifuged for 15 min at 5 °C, at 4500 rpm (centrifuge 5430 R with rotor FA-45–30–11, Eppendorf AG, Hamburg, Germany) and the supernatant was recovered and stored on ice before further usage. For the *in vitro* lipolysis, 1.583 g LBF was dispersed in 57 mL of digestion buffer at 37 °C, with stirring at 600 U/min (stirrer level 4) for 10 min. The pH of the medium was adjusted manually after LBF addition and maintained at pH 6.5 using 0.5 M NaOH. Three samples (1 mL) were taken at 2.5, 5, and 10 min from the middle of the vessel. 6 mL of pancreatin extract (~1000 TBU/mL of digest) was added to the remaining 54 mL dispersion media (containing 1.5 g lipid formulation) to start the digestion process. During the digestion pH was maintained at 6.5 using 0.2 M NaOH for the type IV formulation and 0.6 M NaOH for the other formulations. Samples of 3.335 mL were taken from the middle of the vessel at 5, 10, 15, 30, 45, and 60 min during the digestion experiment. In each sample the enzymes were inhibited by the addition of 1 M 4-Bromophenylboronic acid in methanol (5 µL per mL sample). After 60 min of digestion, the pH was titrated back to pH 9.0 to allow for a determination of released nonionised free FAs.

The samples from the dispersion were centrifuged at 37 °C and 21,000 g for 30 min using a benchtop centrifuge (centrifuge 5430 R with rotor FA-45–30–11, Eppendorf AG, Hamburg, Germany). Samples taken during the digestion were transferred into a centrifugation tube (Quick-Seal® Bell-Top, Beckman Coulter). All digestion samples were centrifuged at 37 °C and 100,000 rpm for 30 min (Optima™ MAX-XP, rotor TLA-110, Beckman Coulter, Brea, USA). Samples that were awaiting centrifugation were stored at 37 °C. After the ultracentrifugation, a sample of the aqueous phase was extracted using a needle and syringe by piercing the tube in the middle, avoiding the sampling of any solid or lipidic content. The obtained samples of the aqueous phase were diluted 1:1 with a mixture of acetonitrile and methanol (35:30, v/v). Subsequently, the top part of the tube was cut open to remove the lipid and aqueous phase. After the liquid was removed, the lowest part of the tube that included the pellet, was cut out. The pellet was dissolved in 5 mL of acetonitrile and ethyl acetate (1:3, v/v). Followed by a 1:10 dilution with a mixture of acetonitrile and ethyl acetate (3:1, v/v). In a third dilution step, the samples were further diluted with mobile phase prior HPLC analysis.

A blank *in vitro* lipolysis experiment was carried out since the biorelevant digestion media contained substances like phospholipids that also get digested and will release FFAs. The quantity of FFAs that were solely liberated during the digestion of FaSSIF was measured in this experiment and used to correct the data obtained for the LBFs. The concentration of nilotinib in the solid and aqueous phase was determined by reverse phase HPLC utilizing a 1260 Infinity series HPLC system (Agilent Technologies, Santa Clara, *CA*, USA) series comprising a quaternary pump, an Agilent autosampler, a thermostat, a thermostated column compartment, and an Agilent Diode Array Detector VL. A Zorbax® Eclipse Plus-C18 column (5 µm, 4.6 mm x 150 mm) was used. The temperature of the column oven and autosampler was set to 25 °C, respectively. The run time was 7 min using an isocratic method with 35 % ACN, 30 % Methanol, 35 % water + 0.1 % triethylamine as mobile phase at a flow rate of 1.5 mL/min. The injection volume was 40 µL and nilotinib was detected at a wavelength of 267 nm. The lower limit of detection (LOD) and lower limit of quantification (LOQ) were 12 ng/mL and 37 ng/mL, respectively, based on the standard error of y-intercept in accordance with the ICH Q2 guideline. The amount in the lipid phase was computed by deducting the quantity of drug in the pellet and aqueous phase samples from the total amount of drug present in the experiment, as the lipid phases were too small to be extracted effectively. To determine the lipase activity of the pancreatin extract, the established protocol of the tributyrin assay by Grundy et al. (2021) was used.

Table 1
Summary of the tested formulations in this study (LC: long-chain and MC: medium-chain).

Excipients [% in w/w]	Lipid type	Formulation code			
		Type I	sLBF	Type III	Type IV
Peceol®	LC	100	100	–	–
Tricaprin	MC	–	–	40	–
Cremophor® RH40	–	–	–	20	33
Tween® 85	–	–	–	40	67

2.2.5. pH-shift in vitro lipolysis model

In vitro lipolysis was performed using a Titrando® 907 (Metrohm AG, Herisau, Switzerland), comprising a pH electrode (Metrohm) and two 800 Dosino® dosing units. The system was operated by the Tiamo® 3.0 software. The pH-shift *in vitro* lipolysis model employed in this study is primarily adapted from the biphasic model described by O'Dwyer et al. (2020). The volumetric parameters and buffer compositions were further refined based on the Dissolution-Transfer-Partitioning System (DTPS) developed by Jede et al. (2023). A schematic representation of the adapted set-up is illustrated in Fig. 1 and a summary of the

experimental conditions is listed in Table 2. The standard dissolution USP II vessel of 1000 mL was filled with 250 mL of SGF pH 2.0 (described in Section 2.2.1) at 37 °C and stirring was initiated at 250 rpm. According to a ratio of 1:200 (LBF:digestion medium) 2.5 g of LBF was subsequently added, using a syringe (Bennett-Lenane et al., 2021). From the middle of the vessel, a 4 mL sample of the dispersion was taken after 15 min. After 29 min, 239 mL of FaSSIF, prepared with double-concentrated phosphate buffer, was added to the dispersion, followed by the addition of 11 mL of pancreatin extract (~1000 TBU/mL of digest), which was then stirred for an additional minute at 250 rpm. The preparation of the pancreatin was done as described in Section 2.2.4. Subsequently, the stirring was decreased to 75 rpm and titration initiated. At the end of the experiment, the released nonionized free fatty acids were determined by a pH increase of the buffer to pH 9.0. A blank *in vitro* lipolysis experiment was carried out to determine the FFAs that were released due to the digestion of FaSSIF. Samples of 4 mL were taken at 2.5, 5, 10, 15, 30, 45, 60, 90, 120 and 180 min during the digestion experiment from the middle of the vessel and inhibited by addition of 1 M 4-Bromophenylboronic acid in methanol (5 µL per mL sample). 3.335 mL of the sample was filled into a centrifugation tube, the rest was collected and checked for the total nilotinib concentration in the sample. To do this, 100 µL of the sample was taken and diluted 1:10 with a mixture of acetonitrile and methanol (35:30, v/v). The samples taken during the dispersion and digestion were ultracentrifuged, diluted and analysed as described in Section 2.2.4.

2.3. *In vivo rat study and bioanalysis*

The *in vivo* pharmacokinetic data used in this study were generated as part of a larger research study investigating various nilotinib formulations. Within this broader study, unpublished data were used to assess the sLBF and type III formulation. The data of the type I suspension (Koehl et al., 2019) and the type IV formulation (Koehl et al., 2020c) were published in previous studies. Additionally, nilotinib was administered in an intravenous formulation to allow the determination of the absolute bioavailability (Koehl et al., 2020b). The protocol used for the study was approved by the institutional animal ethics committee in accordance with Belgian law regulating experiments on animals and in compliance with EC directive 2010/63/EU and the NIH guidelines on animal welfare. The study was conducted using male Sprague Dawley rats weighing between 280-320 g on the day of experiment purchased from Charles River Laboratories Deutschland (Sulzfeld, Germany) and maintained on standard food and water *ad libitum* in the laboratory for at least 5 days prior entering the experiment. Food was removed 16–20 h before dosing and water was available *ad libitum* at all times. Parallel groups of these animals received each formulation via oral gavage at a volume of 2 mL/kg, with a nilotinib dose of 20 mg/kg. Blood samples (200 µL) were collected at 0.5, 1, 2, 4, 6, 8, 10 and 24 h in tubes containing potassium EDTA. Plasma was harvested immediately through centrifugation for 10 min at 1000 g and stored at −80 °C until analysis. Upon completion of the experiment, the animals were euthanized.

Table 2
Experimental conditions of the *in vitro* lipolysis set-ups.

Condition	Standard pH-stat	pH-shift lipolysis
Volume of SGF pH 2.0 [mL]	–	250[c]
Volume of FaSSIF 6.5 + pancreatin [mL]	60[a]	250[c]
Pancreatin [TBU/mL]	~1000	~1000
Reaction vessel	100 mL beaker	USP II vessel (1000 mL)
LBF added [g]	1.583[a]	2.5
Concentration of nilotinib in LBF [mg/mL]	10	10
Lipid load (LBF:digestion medium)	1:40[a,b]	1:200[d]
Stirring speed during dispersion	600 U/min (stirrer level 4)	250 rpm[e]
Stirring speed during digestion	600 U/min (stirrer level 4)	75 rpm[c]

[a] Koehl et al. (2019).
[b] Williams et al. (2012b).
[c] Jede et al. (2023).
[d] based on findings of Bennett-Lenane et al. (2021).
[e] O'Dwyer et al. (2020), maximum stirring speed of USP apparatus.

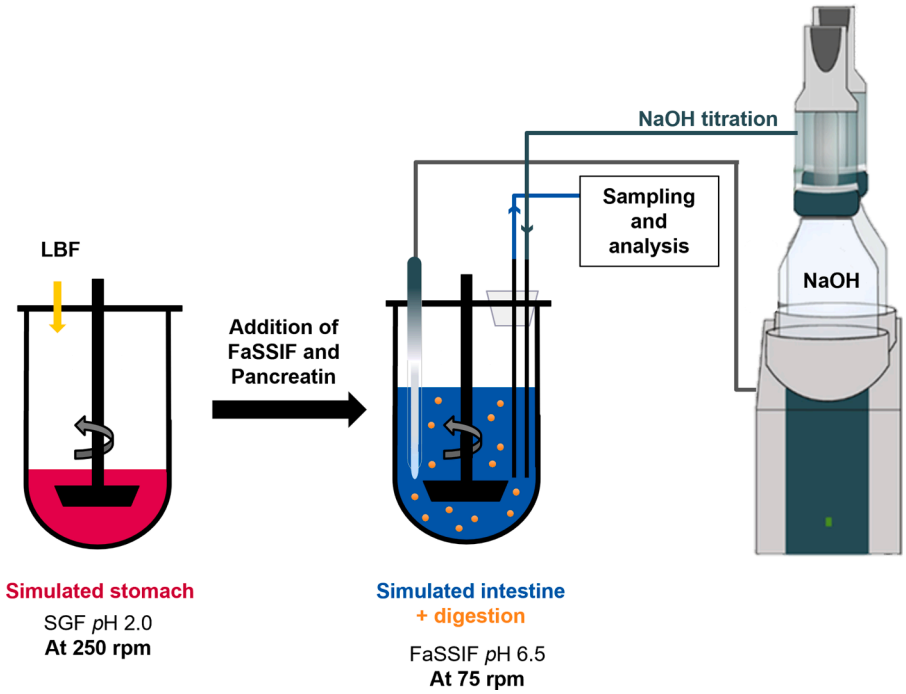

Fig. 1. Schematic representation of the pH-shift *in vitro* lipolysis model. The LBF was added into 250 mL of SGF which was stirred at 250 rpm. After 29 min of dispersion, 250 mL of FaSSIF plus pancreatin extract were added to the vessel. At 30 min the stirring speed was reduced to 75 rpm. The pH-stat instrument maintained a pH of 6.5 during the digestion experiments.

The plasma concentration was determined as described by Koehl et al. (2019). In brief, a Zorbax Eclipse Plus-C18 column (5 µm, 4.6 mm x 150 mm) with a Zorbax Eclipse Plus-C18 guard column (5 µm, 4.6 mm x 12.5 mm) was used on an Agilent 1260 series HPLC system comprising a binary pump, degasser, temperature controlled autosampler, column oven and diode array detector. The mobile phase consisted of water, methanol, acetonitrile and triethylamine (34:30:35:1 v/v) and was used at a flow rate of 0.9 mL/min. The sample and column temperature were set at 5 °C and 25 °C, respectively, and the detection wavelength was 267 nm. Nilotinib was extracted from the plasma samples by liquid-liquid extraction. To 50 µL of the plasma sample 66 µL of a methanol acetonitrile mixture (30:35 v/v), containing 1.25 µg/mL sorafenib as internal standard, was added. The mixture was mixed thoroughly and centrifuged at 22 °C, 11,500 g for 9 min. 50 µL of the supernatant was injected to the HPLC system for analysis. This method's lower limit of quantification (LOQ) was 25 ng/mL (Koehl et al., 2019).

2.4. Data analysis and statistics

2.4.1. In vitro

To calculate the percentage of LBF that was digested, the theoretical amount of FFAs per g of LBF was calculated with Eq. (1). The saponification value (SV) in mg KOH per g of each excipient in the LBF was taken from the certificate of analysis. The molecular weight of KOH is 56.1056 g/mol.

$$Theoretical\ FFA\ [mmol] = \frac{SV\ [mg]}{56.1056\ \left[\frac{g}{mol}\right]} \quad (1)$$

In Eq. (2) the digested % of the LBF was calculated. The total amount (mmol) of FFAs that was released includes the amount that was detected during the titration to pH 9.0.

$$\%\ digested = \frac{released\ FFA\ [mmol]}{theoretical\ FFA\ [mmol]} * 100 \quad (2)$$

Prior to all the analysis the Bartlett́s test was used to check for equal variance. The area under the curves (AUCs) were calculated using the trapezoidal rule. To compare the AUCs and the % digested of the *in vitro* test a one-way ANOVA, followed by a Tukeý s post-hoc test was performed, using GraphPad Prism® 10 (GraphPad Software, USA).

2.4.2. Pharmacokinetic evaluation

The pharmacokinetic parameters were calculated with Microsoft® Excel®. Non-compartmental analysis was used to plot the plasma concentration profiles, and the linear trapezoidal rule was used to calculate each AUC. Absolute bioavailability was calculated using the intravenous data from Koehl et al. (2020b). To compare the absolute bioavailabilities a Welchś one-way Analysis of Variance (ANOVA) test was selected since the variances among the groups were not equal. Following this, a pairwise comparison of the formulations was conducted using Tukeý s multiple comparison test as post-hoc analysis. All statistical analyses were conducted using GraphPad Prism® 10 (GraphPad Software, USA).

2.4.3. In vitro–in vivo relationship (IVIVR)

To evaluate the results from the pH-stat and pH-shift experiments and to allow for an assessment of the predictive power of the *in vitro* models, IVIVR plots were created. *In vitro* data were evaluated based on the dose-normalised AUCs of nilotinib concentration solubilised in the aqueous phase during the digestion, which was considered as the *in vitro* fraction dissolved that was available for absorption. The *in vitro* results were compared with the corresponding *in vivo* dose-normalised $AUCs_{0-10h}$ values of the plasma curves. Since the observed *in vitro* kinetics differed extensively from the *in vivo* plasma profiles, the AUC was chosen instead of the percentage of dose at a certain timepoint. In the pH-stat lipolysis model, the AUC was calculated from the start of the digestion (0-minute sample) until the final sample at 60 min for the IVIVR. For the pH-shift model, the AUC was calculated from the first sample taken at 2.5 min during digestion to subsequent time points at 60, 120 or 180 min.

3. Results

3.1. Solubility in SGF and FaSSIF

The solubility of nilotinib in SGF at pH 2.0 was 117.54 ± 1.70 µg/mL, while in regular prepared FaSSIF (buffer capacity of 10 mmol/L/ΔpH) the solubility was determined to be 0.33 ± 0.02 µg/mL, confirming that solubility of this weakly basic drug decreases at higher pH values. In the double-concentrated FaSSIF, the solubility after 24 h was determined to be 0.59 ± 0.10 µg/mL. It was assumed that the higher chloride ion concentration in the FaSSIF with 10 mmol/L/ΔpH buffer capacity affected the solubility of the ionised form, resulting in lower solubility of nilotinib compared to the solubility in FaSSIF with 20 mmol/L/ΔpH buffer capacity, which contained fewer chloride ions.

3.2. Drug distribution during in vitro pH-stat lipolysis

Among the four formulations tested in the *in vitro* pH-stat lipolysis, the sLBF demonstrated the highest levels of nilotinib in the aqueous phase during digestion, reaching up to 6.0 % of the total dose (Fig. 2). This represents a 7-to 26-fold increase over nilotinib's equilibrium solubility in FaSSIF. The type III suspension also showed effective performance as well, initially showing a decline in solubilized drug but recovering by 30-45 min, with 4.4 % of the dose present in the aqueous phase. In contrast, the type I lipid suspension with Peceol® maintained <1 % of the dose in the aqueous phase throughout digestion (Fig. 2). The Type IV suspension showed the most rapid loss of solubilization, dropping from an average of 8-10 % during dispersion to just 0.1 % after 60 min of digestion, below nilotinib's equilibrium solubility in FaSSIF, indicating poor retention of drug in solution during digestion.

Analysis of the LBFs used in the *in vitro* experiments revealed distinct differences in drug distribution. In the supersaturated LBF (sLBF), nilotinib was fully solubilized within the lipid phase. In contrast, over 85 % of the drug remained as undissolved solid particles in the three suspension-based formulations (Figure 3 A–D). As illustrated in Fig. 3A, the sLBF retained most of the drug in the lipid phase during early digestion, with >75 % remaining solubilized in this reservoir in the first 30 min and minimal drug present in the solid phase. The Type III formulation exhibited a more dynamic drug distribution, with a significant shift of nilotinib from the lipid phase into the solid phase—from 38 % after 5 min digestion to > 80 % after 60 min—indicating notable digestion induced precipitation (Fig. 3B). The type IV LBF, lacking a lipid phase entirely, showed consistently high levels of drug in the solid phase across all time points, confirming its limited ability to maintain drug solubilization during digestion (Fig. 3C). Comparing type III and IV, the findings were consistent with established knowledge that incorporating soluble triglycerides, whether medium-chain or long-chain, can help mitigate the precipitation risk for nilotinib (Mu et al., 2013). The Type I Peceol® suspension initially showed a high proportion of drug in the solid phase, but by 60 min, a shift toward the lipid phase was observed, with only about 30 % of the drug remaining in the pellet (Fig. 3D).

The total amount of released FFAs over 60 min of digestion followed the rank order type III > type *I* ≥ sLBF > type IV (see Fig. 4). For both type I and the type III LBF, oil phases were observed after centrifugation which indicated that the LBFs were only partially digested. Notably, type III LBF exhibited the highest quantity of 52.7 ± 4.1 % since this LBF consisted of MC lipids, while type IV showed the lowest percentage digested at 0.6 ± 4.1 %, consistent with its oil-free composition. Additionally, there was no significant difference in the percentage of digestion between sLBF (20.3 ± 8.4 %) and type I suspension (24.8 ± 7.2 %) with a p-value of 0.818, which was anticipated as both formulations

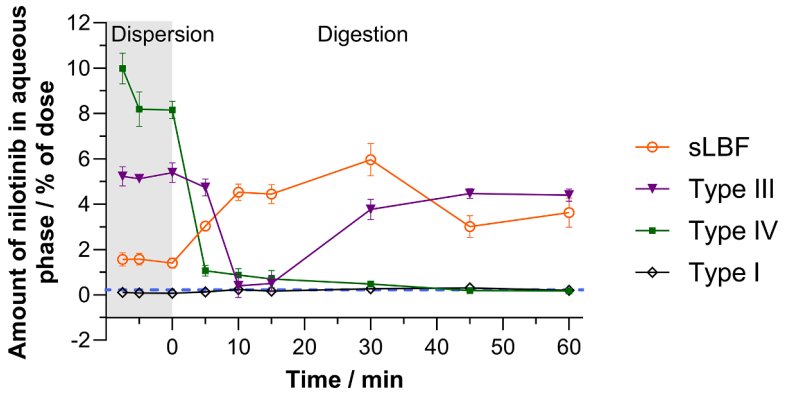

Fig. 2. Percent of nilotinib in the aqueous phase during *in vitro* lipolysis of selected nilotinib LBFs: type IV (■), type III (▼), sLBF (○), type I (◇) (mean ± SD, with n = 3 except for type I −7.5- and −5-min n = 2). The blue dotted line displays the saturated solubility of nilotinib in FaSSIF.

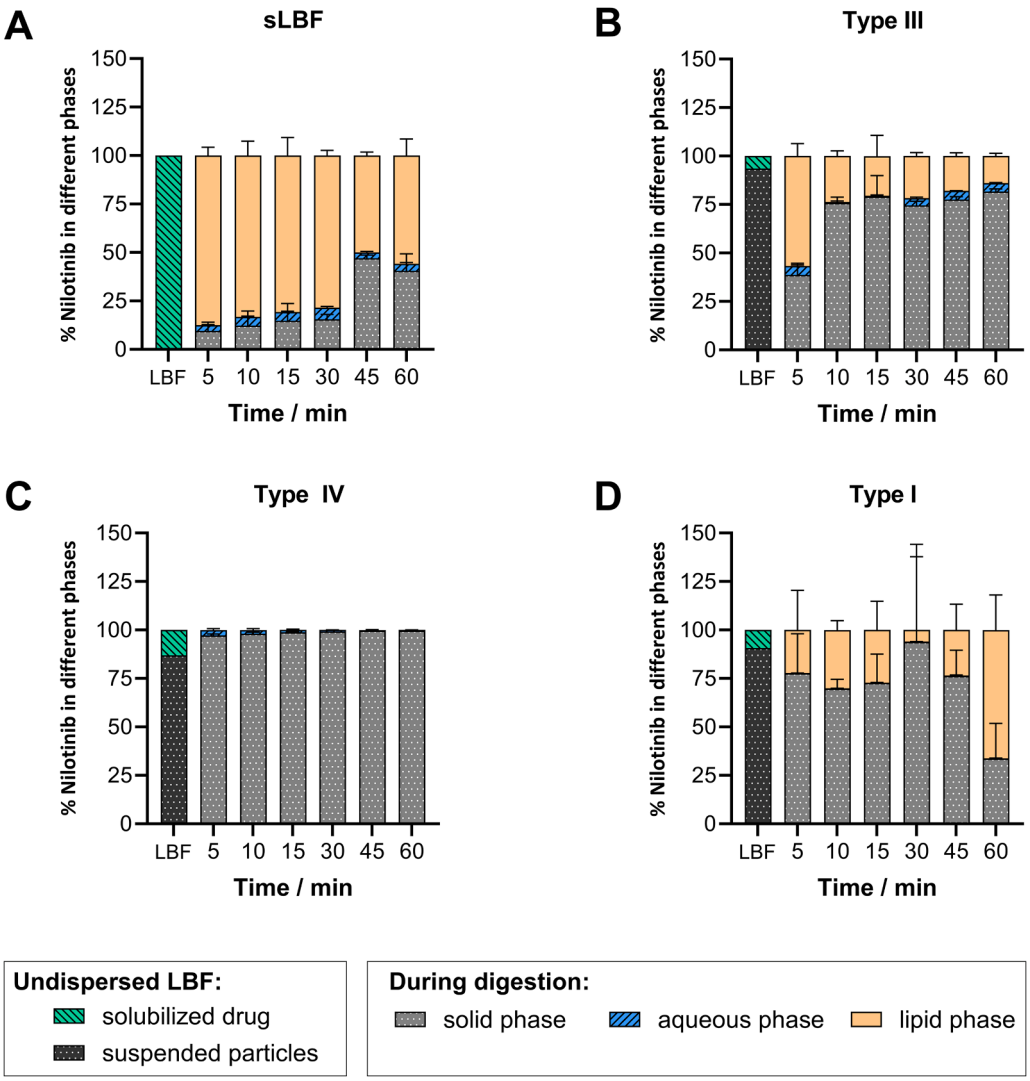

Fig. 3. Distribution of nilotinib in the LBF before dosing, solubilized drug (green, striped) and suspended particles (dark grey, white dotted). Distribution of nilotinib across the solid (grey, white dotted), aqueous (blue, striped) and lipid (light orange) phase during digestion in the pH-stat lipolysis model based on the recovery in these phases. Except the lipid phase, which was calculated by subtracting the sum of recovery in solid and aqueous phase from total theoretical amount of nilotinib. Shown for the formulations **A**: sLBF, **B**: Type III, **C**: Type IV and **D**: Type I. The experiments were run with n = 3 and results are shown as mean + SD.

contained identical quantities of Peceol®. The low digestibility of Peceol® supported the findings reported by Koehl et al. (2020a). Furthermore, for type III, a delay of approximately 15 min was observed after the initiation of digestion before a rapid onset of digestion and a high rate of FFA release in the media occurred. The delay was likely caused by the two surfactants in the type III LBF acting as competitive

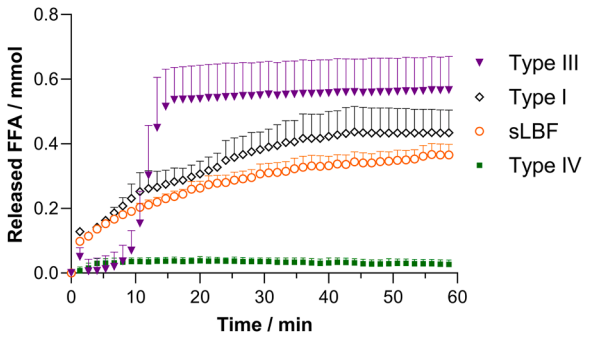

Fig. 4. Free fatty acids (mmol) released over time for the LBFs of interest, during 60 min of digestion of type IV (■), type III (▼), sLBF (○) and type I (◇). The values are corrected for the level of FFA released in background lipolysis (digestion media alone). Every 15th data point is shown in the graph (*i.e.*, a data point every 1 min) to improve graph legibility. Results are shown as mean + SD, $n = 3$.

inhibitors for pancreatic lipase. This mechanism would align with previous findings that PEG-ylated surfactants like Cremophor® RH40 can inhibit digestion by pancreatic enzymes, a behavior also expected for Tween® 85 (Christiansen et al., 2010; Li and McClements, 2011).

3.3. pH-shift in vitro lipolysis model: impact of the additional simulated gastric step

The results of the pH-shift lipolysis model are depicted in Fig. 5 and Fig. 6, which illustrates the release of nilotinib in the aqueous phase and the distribution across the phases throughout digestion, respectively. During dispersion in SGF, the sLBF, type III, and type IV LBFs achieved solubility levels exceeding 80 % of the dose in the aqueous phase. In case of the type I suspension, an average of only 23.0 % of the dose was dissolved in SGF. The sLBF demonstrated an initial 2.5 % of dose in the aqueous phase after 5 min of digestion, followed by a gradual increase that peaked at 5.3 % after 120 min. This formulation demonstrated exceptional stability and solubilization capacity, even under the challenging conditions of pH-shift and prolonged digestion time. The type III LBF exhibited an average of 51.7 % of the added dose in the aqueous phase at 2.5 min, which decreased to 0.8 % at 30 min of digestion. Notably, the increase in solubility during digestion for the type III LBF began later than for the other formulations, with the first increase observed after 45 min. Followed by a second increase, reaching an average of 11.4 % of dose of solubilized drug after 180 min (see Fig. 5). For the Type IV LBF, rapid precipitation occurred on transitioning into intestinal digestion conditions. Whole nilotinib concentrations remained transiently elevated for up to 10 min at ~ 5.4 % of the solubilized dose, the concentration subsequently declined thereafter, stabilizing between 1.3 % and 2.1 % for the remainder of the digestion period. With that the

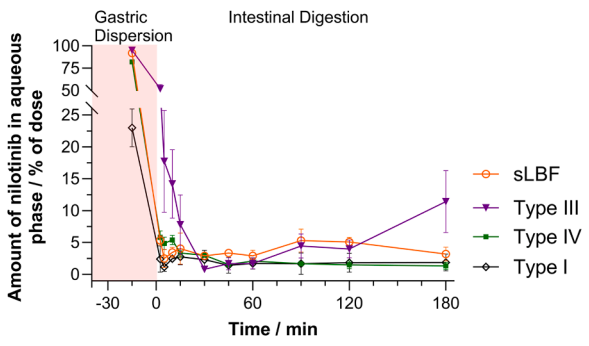

Fig. 5. Percent of nilotinib *in vitro* in the aqueous phase during the pH-shift lipolysis of type IV (■), type III (▼), sLBF (○) and type I (◇) (mean ± SD, with $n = 3$).

type IV formulation demonstrated a high propensity of precipitation during *in vitro* lipolysis, which aligns with previous findings for danazol and fenofibrate (Griffin et al., 2014; Williams et al., 2012a), suggesting a common challenge for surfactant-based formulations of poorly water-soluble drugs. For the type I suspension, rapid precipitation occurred with the pH-shift, with only 1.2 % of the dose remaining solubilized in the aqueous phase. After 10 min, the solubility increased to an average of 2.5 %, but throughout the last 120 min of digestion, the solubilized amount in the aqueous phase remained relatively constant at approximately 1.7 %.

Fig. 6A indicates that the sLBF consistently maintained between 48 and 58 % of dose in the lipid phase, with a consistent amount of drug precipitated during the digestion. Whereas the type III formulation exhibited a more dynamic distribution among the three phases, with a less rapid precipitation observed at the start of digestion compared to the other formulations (Figure 6 B). The solid phase peaked at 44.0 % of the dose at 45 min. For LBF type IV, the onset of digestion was characterised by sudden precipitation (Figure 6 C), notably lacking a lipid phase. The type I suspension, as shown in Figure 6 D, retained 77.0 % of dose in the lipid phase during digestion. Upon the initiation of digestion, rapid precipitation occurred, yet between 60.7-71.5 % of the dose remained in the lipid phase through digestion.

The amount of released FFAs during digestion is illustrated in Fig. 7, revealing that the total FFAs titrated over 180 min of digestion followed the rank order type III > sLBF ≥ type *I* > type IV. Notably, the type III LBF exhibited the highest extent of digestion, achieving 74.7 ± 0.6 %, while the type IV suspension showed the lowest percentage at 5.5 ± 0.2 %. The type I suspension was digested to 15.4 ± 0.3 %, and the sLBF reached a digestion level of 18.1 ± 5.4 %. The release profile of FFAs for type III was distinctive, characterized by a significant increase in FFA release beginning after 5 min, followed by a plateau between 7-10 min, and a subsequent rapid surge after 10 min. This delayed release of FFAs aligns with the observation made with the pH-stat model (see Section 3.2). In contrast, the formulations containing Peceol® exhibited a rapid increase in FFA release in the initial 20 min, which was followed by a gradual decline in the rate of release over time.

3.4. Pharmacokinetic study

The *in vivo* performance of four LBFs, listed in Table 1 (Section 2.2.3), was evaluated in male Sprague Dawley rats. The pharmacokinetic profiles and calculated parameters are presented in Fig. 8A and Table 3, respectively. The plasma concentration profiles for Peceol® and the Type IV LFC suspension have been reported previously (Koehl et al., 2019, 2020c). All formulations were administered at a fixed dose of 20 mg/kg nilotinib and a lipid volume of 2 mL/kg. The sLBF and type III formulation demonstrated notably higher plasma concentrations throughout the 10-hour observation period compared to the type IV and type I suspensions. The sLBF achieved the highest mean plasma concentration, with a maximum plasma concentration (c_{max}) of 7.79 ± 1.85 µg/mL, at 2 h (t_{max}). In contrast, the Type III formulation exhibited a markedly slower absorption profile. This pattern aligns well with the delayed released FFAs measured observed in both *in vitro* models (see Sections 3.2 and 3.3). The c_{max} for this formulation was 6.84 ± 2.13 µg/mL, achieved at a later t_{max} of 6 h. Both the type I suspension and the type IV suspension reached their maximum plasma concentration after 4 h, with average values between 2.8–2.9 µg/mL.

As displayed in Fig. 8 and Table 3, the sLBF demonstrated the highest AUC_{0-10h} at around 62 ± 17 µg*h/mL. This was followed by the self-emulsifying type III LBF suspension, which exhibited an average of 52 ± 20 µg*h/mL. The type IV suspension achieved an AUC_{0-10h} of approximately 17 ± 6 µg*h/mL, while the type I suspension demonstrated a lower AUC_{0-10h} of around 12 ± 3 µg*h/mL. When comparing the type I Peceol® suspension to the supersaturated LBF, both compositionally equivalent in terms of Peceol® content, the sLBF demonstrated a six-fold higher bioavailability. This underscores the critical role of the

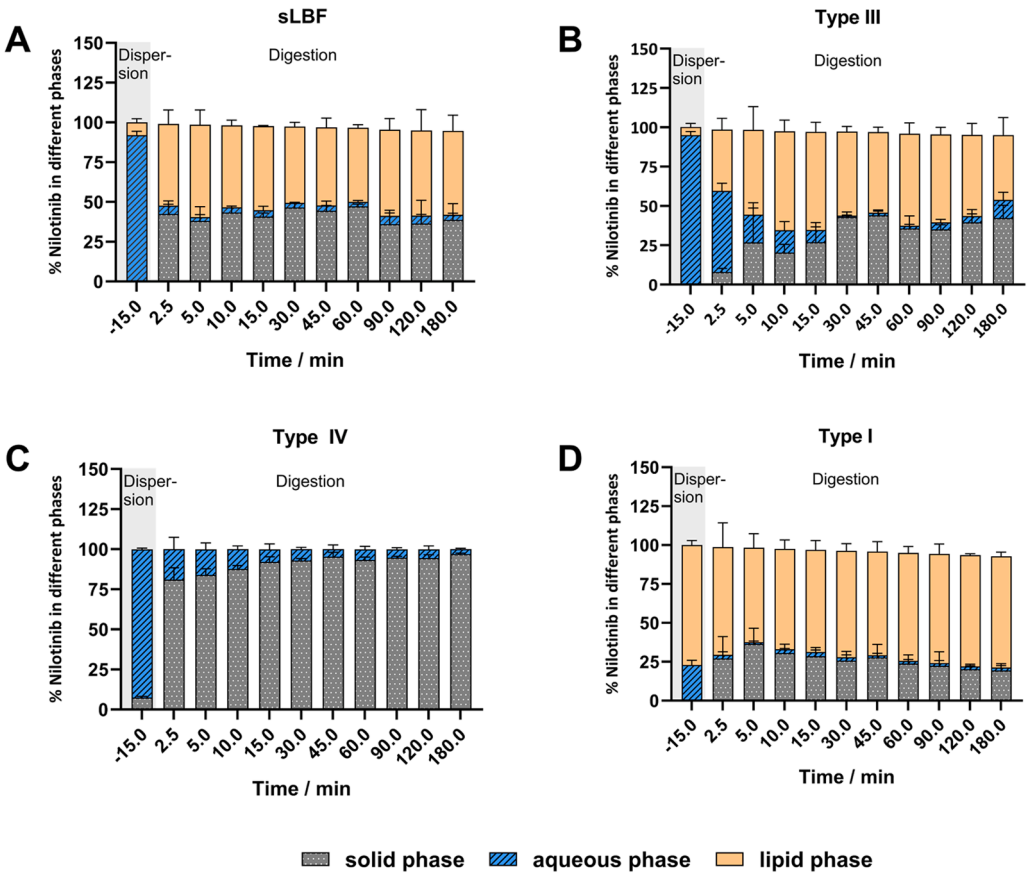

Fig. 6. Distribution of nilotinib across the solid (grey, white dotted), aqueous (blue, striped) and lipid (light orange) phase during digestion in the pH-shift lipolysis model based on the recovery in these phases. Except the lipid phase, which was calculated by subtracting the sum of recovery in solid and aqueous phase from total theoretical amount of nilotinib. Shown for the formulations **A**: sLBF, **B**: Type III, **C**: Type IV and **D**: Type I. The experiments were run with $n = 3$ and results are shown as mean + SD.

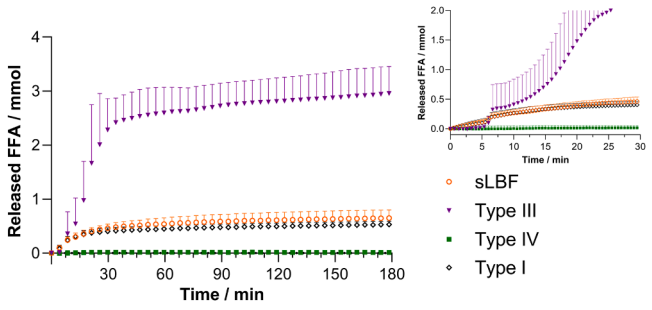

Fig. 7. Free fatty acids (mmol) released over time for the LBFs of interest in the pH-shift lipolysis model, during 180 min of digestion of type IV (■), type III (▼), sLBF (○) and type I (◇). The values are corrected for the level of FFA released in background lipolysis (digestion media alone). Every 50th data point is shown in the graph (*i.e.*, a data point every 4 min on the left, every 30 s on the right) to improve graph legibility. Results are shown as mean + SD, $n = 3$.

supersaturation within the formulation to enhancing the performance of poorly dispersible formulations. Comparing the type III and IV LBF indicated that the combination of lipids and surfactants in the formulation was key for nilotinib to achieving a high *in vivo* exposure.

3.5. *In vitro–in vivo relationships (IVIVRs)*

Fig. 9 shows the calculated IVIVRs, with the highest R-squared values obtained by the standard pH-stat model (Fig. 9A) and the pH-shift model when using the AUC up to 120 min, as illustrated in Fig. 9C. The relationship established with the pH-stat ($R^2 = 0.993$) being slightly better than achieved with the pH-shift method ($R^2 = 0.824$) (Fig. 9). Notably, the standard deviations of the *in vitro* AUC for the pH-shift model were significantly larger compared to those for the pH-stat model. In total Fig. 9 demonstrates a strong positive relationship between *in vivo* AUC and the *in vitro* lipolysis results for both models regardless of the time considered in the pH-shift model.

4. Discussion

LBFs have emerged as a promising formulation strategy to overcome the absorption limitations associated with poorly soluble and poorly permeable small molecules. However, their dynamic behavior during digestion complicates the prediction of *in vivo* performance using current *in vitro* models, which often struggle to establish robust IVIVRs (Berthelsen et al., 2019; Feeney et al., 2016; Huang et al., 2021). This study investigated whether the pH-shift model provided insights into drug release behavior beyond the simpler pH-stat model and if its increased complexity improves IVIVRs. The findings of this research were of significant interest, as they enhance the understanding of formulation performance and contribute to the development of more effective drug delivery systems.

4.1. *sLBF and type III lipid suspension offer increased bioavailability of nilotinib*

Among the four LBFs tested, it was possible to identify a rank order of the formulations based on their average bioavailability, type III ≥ sLBF > type IV ≥ type I (see Section 3.4). In this study the sLBF and type III

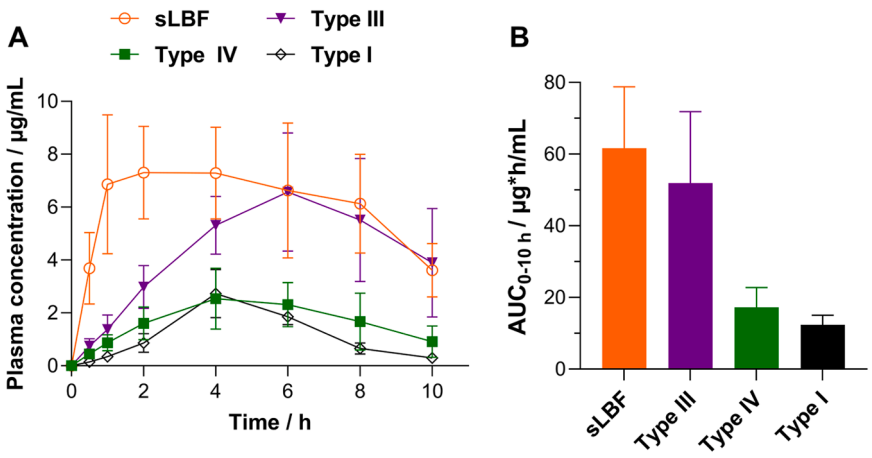

Fig. 8. **A**: Plasma concentration-time profiles as a function of time (mean ± SD, $n = 5$) after oral administration of nilotinib in four tested formulations: type IV (■) (data from Koehl et al., 2020c), type III (▼), sLBF (○) and type I (◇) (data from Koehl et al., 2019) at a dose of 20 mg/kg. The majority of the 24 h samples were below LOQ and hence not depicted. **B**: AUC_{0-10h} of nilotinib in formulations tested in rats: sLBF (orange), type III (purple), type IV (green), and type I (black). The data is shown in mean + SD, with $n = 5$.

Table 3
Pharmacokinetic parameters of nilotinib after oral administration of nilotinib (20 mg/kg) to male Sprague Dawley rats (with $n = 5$). F represents absolute bioavailability. T_{max} given as median (range), all other parameters as mean ± SD, Peceol® (Type I) and Tween® 85/Cremophor® RH40 (Type IV) as published by Koehl, 2020.

	Pharmacokinetic parameters			
	sLBF	**Type III**	**Type IV***	**Type I#**
c_{max} [µg/mL]	7.79 ± 1.85[a]	6.84 ± 2.13[a]	2.93 ± 1.01[b]	2.80 ± 0.76[b]
t_{max} [h] (range)	2 (2–8)	6 (4–8)	4 (2–8)	4 (4–6)
AUC_{0-10h} [µg*h/mL]	61.66 ± 17.14[a]	51.89 ± 19.96[a]	17.25 ± 5.51[b]	12.39 ± 2.67[b]
AUC_{0-inf} [µg*h/mL]	68.49 ± 20.10[a]	74.71 ± 30.62[a]	18.98 ± 6.24[b]	13.63 ± 2.66[b]
F_{0-10h} [%]	55.5 ± 15.4[a]	46.7 ± 18.0[a]	15.5 ± 5.0[b]	11.2 ± 2.4[b]
F [%]	61.6 ± 17.0[a]	67.2 ± 32.5[a]	17.1 ± 5.6[b]	12.3 ± 2.4[b]

a,b Within a row, means without a common superscript differ ($p < 0.05$).
* Data from Koehl et al., 2020c;.
# Data from Koehl et al., 2019.

suspension, demonstrated a 6-fold higher bioavailability compared to the type I and type IV suspension. The performance of the sLBF emphasized that the physical state of the drug in the formulation was crucial for the absorption. In line with other studies for model compounds such as venetoclax (Koehl et al., 2020a), simvastatin (Thomas et al., 2013), and fenofibrate (Thomas et al., 2014) the supersaturated lipid solution showed promising *in vivo* results, where supersaturated lipid solutions outperformed undersaturated formulations in terms of bioavailability enhancement (Ilie et al., 2020). However, it is imperative to acknowledge the inherent challenges associated with supersaturated systems, particularly their limited thermodynamic stability and propensity for precipitation (Holm et al., 2023). These factors have thus far confined the application of supersaturated LBFs to preclinical studies, with no marketed formulations currently available.

In contrast to the oil-only supersaturated systems, lipid suspensions like the type III may offer advantages in terms of stability, scalability and ease of preparation. Nilotinib is classified as a `brick-dust` molecule due to its limited solubility in lipid excipients, rendering classical lipid solutions as not feasible. Consequently, lipid suspensions have primarily been investigated for nilotinib (Koehl et al., 2019). Among the three tested LBF suspensions, the type III formulation demonstrated superior performance in this study, underscoring the synergistic effect of combining oils and surfactants in self-emulsifying systems. These findings further reinforce the growing body of evidence supporting the potential of LBFs to enhance drug exposure. Moreover, they underscore the value of exploring LBFs beyond the traditional LFCS types, in order to fully leverage the benefits of lipid excipients for improving oral drug delivery—particularly for candidates with poor solubility in both aqueous and lipid environments.

4.2. pH-shift offers unique mechanistic insights in case of weakly basic compounds in LBFs

The classical pH-stat model provides insights into the ability of LBFs to aid supersaturation of the drug in the duodenum. In this study, the pH-stat model revealed that the sLBF maintained higher amounts of drug throughout the 60 min of digestion. In contrast, the type IV formulation predominantly retained the drug in the solid phase, while the type I formulation exhibited lipid entrapment, potentially limiting bioavailability. The type III formulation indicated dynamic distribution, with a notable portion of nilotinib transitioning to the solid phase. However, the pH-shift offered more insights into the behavior of the drug as it transitions from stomach to duodenum. The dispersion in SGF of a free base and highly dispersible formulations, such as type IV and type III, benefits from the higher solubility of the free drug in acidic medium. It captured the entrapment of the drug within the type I suspension during dispersion, which persists throughout digestion. Koehl et al. (2019) reported that the entrapment of nilotinib crystals within lipidic excipients during digestion contributed to delayed drug release due to the poor dispersibility of the formulations, ultimately leading to reduced absorption. With the transition from SGF to intestinal digestion media, there was a certain level of precipitation observed in all formulations. The pH-shift model allowed to capture the benefit of the type III during gastric transitioning, after the pH-shift a more transient precipitation was observed than for the other two suspensions. Furthermore, in the standard pH-stat model, a pronounced difference between *in vitro* fraction dissolved and *in vivo* absolute bioavailability was observed. In comparison the pH-shift model was able to achieve higher *in vitro* fraction dissolved, especially for the type I and the type IV suspension (Fig. 2), due to the added gastric step.

4.3. Solid IVIVRs with standard pH-stat and pH-shift lipolysis

In contrast to numerous previous studies where LBFs evaluated using the standard pH-stat model failed to correlate with *in vivo* outcomes (Feeney et al., 2016; Huang et al., 2021), the present study demonstrated that both the pH-stat and pH-shift models established strong and

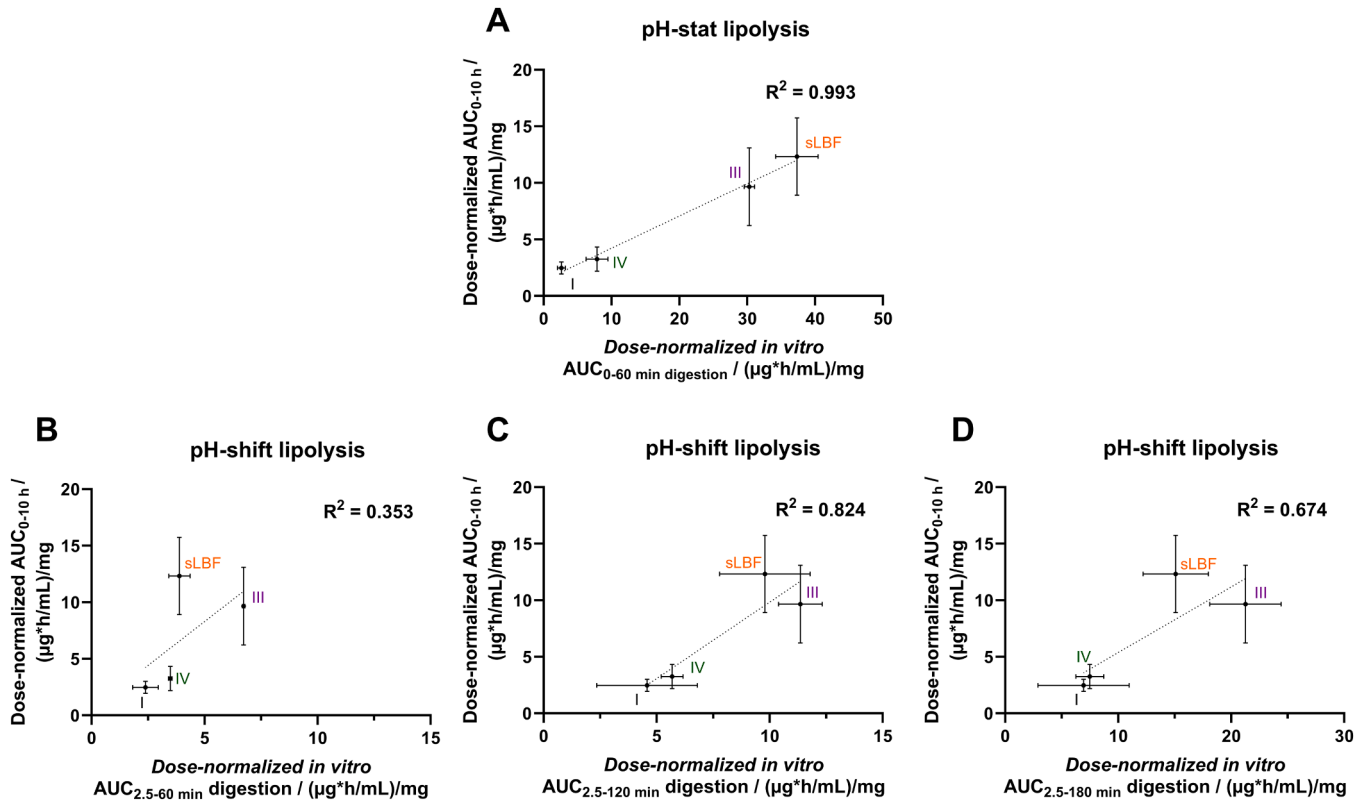

Fig. 9. IVIVR with **A**: AUC of pH-stat lipolysis; **B, C** and **D**: AUC of different time frames of pH-shift lipolysis. Dose-normalized AUC_{0-10h} of *in vivo* exposure is plotted against *in vitro* AUC during digestion (**A**: $AUC_{0-60min;}$ **B**: $AUC_{2.5-60min,}$ **C**: $AUC_{2.5-120min}$ and **D**: $AUC_{2.5-180min}$).

reliable IVIVRs (Fig. 9A). In the pH-shift model, various IVIVRs were evaluated using AUCs from the first sample taken during digestion to 60, 120 or 180 min (Fig. 9B-D). Considering the R^2 values, the AUCs including 120 min of digestion are the most relevant. This aligns with findings from Steingoetter et al. (2019) that, in their *in vivo* rat study, the plasma concentration of FFAs reached their maximum within the first 2 h following gastric ingestion of lipids.

A key methodological consideration was the initial dispersion of formulations at 250 rpm to ensure uniform dispersion across the range of formulations. This approach was considered necessary to ensure the 4 types of formulations were consistently dispersed and to accurately study the impact of the pH-shift. A practical explanation for why a digestion time longer than 60 min was necessary in the pH-shift experiment was the reduced stirring rate, which was lowered to 75 rpm, significantly lower than the stirring rate in the pH-stat model. Wu and Tsai (2004) demonstrated that the specific activity of free lipases increased with higher shaking rates, as the reaction was influenced by the mass transfer of lipase from the bulk solution to the interfacial area of the lipid droplets. Moreover, the substrate concentration in the pH-shift model, which was 5 mg/mL of lipids in digestion medium, was lower than in the pH-stat experiment, where the concentration was 25 mg/mL, further impacting reaction kinetics. The R^2 when considering 180 min of digestion compared to the extended 120 min period was lower. This is primarily attributed to the type III LBF, which exhibited an anomalous increase in aqueous phase drug concentration after 120 min. This increase was not associated with further lipid digestion, as evidenced by the NaOH titration data remaining constant during this period. The observed phenomenon suggests a complex, time-dependent solubilization process that is not directly linked to ongoing lipolysis.

While this study demonstrated promising results for both the pH-stat and pH-shift lipolysis models with nilotinib LBFs, further research is necessary to fully elucidate the potential advantages of the pH-shift model. A limitation of both models is their lack of simulating sink conditions, which restricts the ability to gain insights into absorption mechanisms. To address this issue, one potential strategy could involve adding an absorptive layer to the experimental setup of the pH-shift model, which would help maintain sink conditions throughout the digestion process and potentially reduce the extent of drug precipitation (O'Dwyer et al., 2020).

5. Conclusions

This study assessed the performance of LBFs containing nilotinib by comparing *in vivo* pharmacokinetic outcomes with predictions from two *in vitro* models: the standard pH-stat lipolysis model and a more complex pH-shift system. This head-to-head comparison provided valuable insights into how model complexity influences the predictive power of *in vitro* assessments. Both models demonstrated positive IVIVRs, with type III LBF and sLBF clustering together and outperforming the type I and type IV suspensions, showing similar lower performance levels. The pH-shift model offered enhanced mechanistic understanding of nilotinib's precipitation behavior during simulated gastrointestinal transit, making it particularly useful for formulation development of weakly basic drugs. The choice between the two models should be guided by the specific objectives of the scientific question. Accordingly, the standard pH-stat model is suitable for early-stage development when material consumption needs to be minimized, and rapid assessments are required. In contrast, the pH-shift model, while more complex and resource-intensive, has the potential to provide deeper insights into the formulation's behavior and can be particularly valuable in later stages of formulation development. Future research should validate these *in vitro* lipolysis models with a broader range of drugs and/or formulations to improve the understanding of their applicability during pharmaceutical development.

Declaration of generative AI and AI-assisted technologies

During the preparation of this work the author used (MyGPT-suite/ Merck KGaA) to improve readability and language. After using this tool, the author reviewed and edited the content as needed and takes full responsibility for the content of the publication.

CRediT authorship contribution statement

Hannah S. Kirschbaum: Writing – review & editing, Writing – original draft, Visualization, Validation, Project administration, Methodology, Investigation, Formal analysis, Conceptualization. **Niklas J. Koehl:** Writing – review & editing, Validation, Methodology, Data curation, Conceptualization. **Johannes A. Blechar:** Writing – review & editing, Validation, Supervision, Resources, Project administration, Methodology, Conceptualization. **Christina Wiesinger:** Methodology, Investigation. **Laura J. Koehl:** Writing – review & editing, Visualization, Validation, Supervision, Methodology, Conceptualization. **Patrick J. ODwyer:** Writing – review & editing, Validation, Supervision, Methodology, Conceptualization. **Martin Kuentz:** Writing – review & editing, Validation, Supervision, Methodology, Conceptualization. **René Holm:** Writing – review & editing, Validation, Supervision, Resources, Methodology, Investigation, Conceptualization. **Christian Jede:** Writing – review & editing, Validation, Supervision, Resources, Project administration, Methodology, Conceptualization. **Brendan T. Griffin:** Writing – review & editing, Validation, Supervision, Methodology, Conceptualization.

Declaration of competing interest

The authors declare no conflict of interest related to this article.

Acknowledgements

Part of this work was kindly supported by funding from the Horizon 2020 Marie Sklodowska-Curie Innovative Training Networks programme under grant agreement No 674909.

Supplementary materials

Supplementary material associated with this article can be found, in the online version, at doi:10.1016/j.ejps.2025.107250.

Data availability

Data will be made available on request.

References

Bennett-Lenane, H., Jorgensen, J.R., Koehl, N.J., Henze, L.J., O'Shea, J.P., Mullertz, A., Griffin, B.T., 2021. Exploring porcine gastric and intestinal fluids using microscopic and solubility estimates: impact of placebo self-emulsifying drug delivery system administration to inform bio-predictive *in vitro* tools. Eur. J. Pharm. Sci. 161, 105778. https://doi.org/10.1016/j.ejps.2021.105778.

Berthelsen, R., Klitgaard, M., Rades, T., Mullertz, A., 2019. *In vitro* digestion models to evaluate lipid based drug delivery systems; present status and current trends. Adv. Drug Deliv. Rev. 142, 35–49. https://doi.org/10.1016/j.addr.2019.06.010.

Christiansen, A., Backensfeld, T., Weitschies, W., 2010. Effects of non-ionic surfactants on *in vitro* triglyceride digestion and their susceptibility to digestion by pancreatic enzymes. Eur. J. Pharm. Sci. 41, 376–382. https://doi.org/10.1016/j.ejps.2010.07.005.

Ejskjaer, L., O'Dwyer, P.J., Ryan, C.D., Holm, R., Kuentz, M., Box, K.J., Griffin, B.T., 2024. Developing an *in vitro* lipolysis model for real-time analysis of drug concentrations during digestion of lipid-based formulations. Eur. J. Pharm. Sci. 194, 106681. https://doi.org/10.1016/j.ejps.2023.106681.

FDA, Nilotinib (Tagsigna)-clinical pharmacology and biopharmaceutics review, p. Accessed December 29th 2023, https://www.accessdata.fda.gov/drugsatfda_docs/nda/2007/022068s000_ClinPharmR.pdf.

Feeney, O.M., Crum, M.F., McEvoy, C.L., Trevaskis, N.L., Williams, H.D., Pouton, C.W., Charman, W.N., Bergstrom, C.A.S., Porter, C.J.H., 2016. 50years of oral lipid-based formulations: provenance, progress and future perspectives. Adv. Drug Deliv. Rev. 101, 167–194. https://doi.org/10.1016/j.addr.2016.04.007.

Griffin, B.T., Kuentz, M., Vertzoni, M., Kostewicz, E.S., Fei, Y., Faisal, W., Stillhart, C., O'Driscoll, C.M., Reppas, C., Dressman, J.B., 2014. Comparison of *in vitro* tests at various levels of complexity for the prediction of *in vivo* performance of lipid-based formulations: case studies with fenofibrate. Eur. J. Pharm. Biopharm. 86, 427–437. https://doi.org/10.1016/j.ejpb.2013.10.016.

Grundy, M.M.L., Abrahamse, E., Almgren, A., Alminger, M., Andres, A., Ariëns, R.M.C., Bastiaan-Net, S., Bourlieu-Lacanal, C., Brodkorb, A., Bronze, M.R., Comi, I., Couëdelo, L., Dupont, D., Durand, A., El, S.N., Grauwet, T., Heerup, C., Heredia, A., Infantes Garcia, M.R., Jungnickel, C., Kłosowska-Chomiczewska, I.E., Létisse, M., Macierzanka, A., Mackie, A.R., McClements, D.J., Menard, O., Meynier, A., Michalski, M.-C., Mulet-Cabero, A.-I., Mullertz, A., Payeras Perelló, F.M., Peinado, I., Robert, M., Secouard, S., Serra, A.T., Silva, S.D., Thomassen, G., Tullberg, C., Undeland, I., Vaysse, C., Vegarud, G.E., Verkempinck, S.H.E., Viau, M., Zahir, M., Zhang, R., Carrière, F., 2021. INFOGEST inter-laboratory recommendations for assaying gastric and pancreatic lipases activities prior to in vitro digestion studies. J. Funct. Foods. 82. https://doi.org/10.1016/j.jff.2021.104497.

Holm, R., Kuentz, M., Ilie-Spiridon, A.R., Griffin, B.T., 2023. Lipid based formulations as supersaturating oral delivery systems: from current to future industrial applications. Eur. J. Pharm. Sci. 189, 106556. https://doi.org/10.1016/j.ejps.2023.106556.

Huang, Y., Yu, Q., Chen, Z., Wu, W., Zhu, Q., Lu, Y., 2021. *In vitro* and *in vivo* correlation for lipid-based formulations: current status and future perspectives. Acta Pharm. Sin. B 11, 2469–2487. https://doi.org/10.1016/j.apsb.2021.03.025.

Ilie, A.R., Griffin, B.T., Kolakovic, R., Vertzoni, M., Kuentz, M., Holm, R., 2020. Supersaturated lipid-based drug delivery systems - exploring impact of lipid composition type and drug properties on supersaturability and physical stability. Drug Dev. Ind. Pharm. 46, 356–364. https://doi.org/10.1080/03639045.2020.1721526.

Jede, C., Henze, L.J., Meiners, K., Bogdahn, M., Wedel, M., van Axel, V., 2023. Development and application of a dissolution-transfer-partitioning system (DTPS) for biopharmaceutical drug characterization. Pharmaceutics. 15. https://doi.org/10.3390/pharmaceutics15041069.

Jede, C., Wagner, C., Kubas, H., Weigandt, M., Weber, C., Lecomte, M., Badolo, L., Koziolek, M., Weitschies, W., 2019. Improved prediction of *in vivo* supersaturation and precipitation of poorly soluble weakly basic drugs using a biorelevant bicarbonate buffer in a gastrointestinal transfer model. Mol. Pharm. 16, 3938–3947. https://doi.org/10.1021/acs.molpharmaceut.9b00534.

Klitgaard, M., Beilles, S., Sassene, P.J., Berthelsen, R., Mullertz, A., 2020. Adding a gastric step to the intestinal *In vitro* digestion model improves the prediction of pharmacokinetic data in beagle dogs of two lipid-based drug delivery systems. Mol. Pharm. 17, 3214–3222. https://doi.org/10.1021/acs.molpharmaceut.0c00307.

Klitgaard, M., Mullertz, A., Berthelsen, R., 2021. Estimating the oral absorption from self-nanoemulsifying drug delivery systems using an *In vitro* lipolysis-permeation method. Pharmaceutics. 13. https://doi.org/10.3390/pharmaceutics13040489.

Koehl, N.J., 2020. Exploring the Utility of Lipid-Based Formulation Technology to Enhance Oral Bioavailability of BCS Class IV Molecules. University College Cork, Ireland. https://hdl.handle.net/10468/11419.

Koehl, N.J., Henze, L.J., Kuentz, M., Holm, R., Griffin, B.T., 2020a. Supersaturated lipid-based formulations to enhance the oral bioavailability of Venetoclax. Pharmaceutics. 12. https://doi.org/10.3390/pharmaceutics12060564.

Koehl, N.J., Holm, R., Kuentz, M., Griffin, B.T., 2019. New insights into using lipid based suspensions for 'Brick dust' Molecules: case study of Nilotinib. Pharm. Res. 36, 56. https://doi.org/10.1007/s11095-019-2590-y.

Koehl, N.J., Holm, R., Kuentz, M., Griffin, B.T., 2020b. Chase dosing of lipid formulations to enhance oral bioavailability of Nilotinib in rats. Pharm. Res. 37, 124. https://doi.org/10.1007/s11095-020-02841-9.

Koehl, N.J., Holm, R., Kuentz, M., Jannin, V., Griffin, B.T., 2020c. Exploring the impact of surfactant type and digestion: highly digestible surfactants improve oral bioavailability of Nilotinib. Mol. Pharm. 17, 3202–3213. https://doi.org/10.1021/acs.molpharmaceut.0c00305.

Kostewicz, E.S., Abrahamsson, B., Brewster, M., Brouwers, J., Butler, J., Carlert, S., Dickinson, P.A., Dressman, J., Holm, R., Klein, S., Mann, J., McAllister, M., Minekus, M., Muenster, U., Mullertz, A., Verwei, M., Vertzoni, M., Weitschies, W., Augustijns, P., 2014. *In vitro* models for the prediction of *in vivo* performance of oral dosage forms. Eur. J. Pharm. Sci. 57, 342–366. https://doi.org/10.1016/j.ejps.2013.08.024.

Kuentz, M., 2012. Lipid-based formulations for oral delivery of lipophilic drugs. Drug Discov Today 9, e97–e104. https://doi.org/10.1016/j.ddtec.2012.03.002.

Kuentz, M., Holm, R., Elder, D.P., 2016. Methodology of oral formulation selection in the pharmaceutical industry. Eur. J. Pharm. Sci. 87, 136–163. https://doi.org/10.1016/j.ejps.2015.12.008.

Leuner, C., Dressman, J., 2000. Improving drug solubility for oral delivery using solid dispersions. Europ. J. Pharmac. Biopharmac. 50, 47–60. https://doi.org/10.1016/S0939-6411(00)00076-X.

Li, Y., McClements, D.J., 2011. Inhibition of lipase-catalyzed hydrolysis of emulsified triglyceride oils by low-molecular weight surfactants under simulated gastrointestinal conditions. Eur. J. Pharm. Biopharm. 79, 423–431. https://doi.org/10.1016/j.ejpb.2011.03.019.

Miller, J.M., Beig, A., Krieg, B.J., Carr, R.A., Borchardt, T.B., Amidon, G.E., Amidon, G.L., Dahan, A., 2011. The solubility-permeability interplay: mechanistic modeling and predictive application of the impact of micellar solubilization on intestinal permeation. Mol. Pharm. 8, 1848–1856. https://doi.org/10.1021/mp200181v.

Minekus, M., Alminger, M., Alvito, P., Ballance, S., Bohn, T., Bourlieu, C., Carriere, F., Boutrou, R., Corredig, M., Dupont, D., Dufour, C., Egger, L., Golding, M., Karakaya, S., Kirkhus, B., Le Feunteun, S., Lesmes, U., Macierzanka, A., Mackie, A.,

Marze, S., McClements, D.J., Menard, O., Recio, I., Santos, C.N., Singh, R.P., Vegarud, G.E., Wickham, M.S., Weitschies, W., Brodkorb, A., 2014. A standardised static *in vitro* digestion method suitable for food - an international consensus. Food Funct. 5, 1113–1124. https://doi.org/10.1039/C3FO60702J.

Mu, H., Holm, R., Mullertz, A., 2013. Lipid-based formulations for oral administration of poorly water-soluble drugs. Int. J. Pharm. 453, 215–224. https://doi.org/10.1016/j.ijpharm.2013.03.054.

O'Driscoll, C.M., Griffin, B.T., 2008. Biopharmaceutical challenges associated with drugs with low aqueous solubility-the potential impact of lipid-based formulations. Adv. Drug Deliv. Rev. 60, 617–624. https://doi.org/10.1016/j.addr.2007.10.012.

O'Dwyer, P.J., Box, K.J., Koehl, N.J., Bennett-Lenane, H., Reppas, C., Holm, R., Kuentz, M., Griffin, B.T., 2020. Novel biphasic lipolysis method to predict *in vivo* performance of lipid-based formulations. Mol. Pharm. 17, 3342–3352. https://doi.org/10.1021/acs.molpharmaceut.0c00427.

Porter, C.J., Trevaskis, N.L., Charman, W.N., 2007. Lipids and lipid-based formulations: optimizing the oral delivery of lipophilic drugs. Nat. Rev. Drug Discov. 6, 231–248. https://doi.org/10.1038/nrd2197.

Pouton, C.W., 2006. Formulation of poorly water-soluble drugs for oral administration: physicochemical and physiological issues and the lipid formulation classification system. Europ. J. Pharmac. Sci. 29, 278–287. https://doi.org/10.1016/j.ejps.2006.04.016.

Sek, L., Porter, C.J., Kaukonen, A.M., Charman, W.N., 2002. Evaluation of the in-vitro digestion profiles of long and medium chain glycerides and the phase behaviour of their lipolytic products. J. Pharm. Pharmacol. 54, 29–41. https://doi.org/10.1211/0022357021771896.

Shukla, S., Skoumbourdis, A.P., Walsh, M.J., Hartz, A.M., Fung, K.L., Wu, C.P., Gottesman, M.M., Bauer, B., Thomas, C.J., Ambudkar, S.V., 2011. Synthesis and characterization of a BODIPY conjugate of the BCR-ABL kinase inhibitor Tasigna (nilotinib): evidence for transport of Tasigna and its fluorescent derivative by ABC drug transporters. Mol. Pharm. 8, 1292–1302. https://doi.org/10.1021/mp2001022.

Stegemann, S., Moreton, C., Svanback, S., Box, K., Motte, G., Paudel, A., 2023. Trends in oral small-molecule drug discovery and product development based on product launches before and after the Rule of five. Drug Discov. Today 28, 103344. https://doi.org/10.1016/j.drudis.2022.103344.

Steingoetter, A., Arnold, M., Scheuble, N., Fedele, S., Bertsch, P., Liu, D., Parker, H.L., Langhans, W., Fischer, P., 2019. A rat model of Human lipid emulsion digestion. Front. Nutr. 6, 170. https://doi.org/10.3389/fnut.2019.00170.

Stillhart, C., Imanidis, G., Griffin, B.T., Kuentz, M., 2014. Biopharmaceutical modeling of drug supersaturation during lipid-based formulation digestion considering an absorption sink. Pharm. Res. 31, 3426–3444. https://doi.org/10.1007/s11095-014-1432-1.

Stillhart, C., Kuentz, M., 2016. Trends in the assessment of drug supersaturation and precipitation *In vitro* using lipid-based delivery systems. J. Pharm. Sci. 105, 2468–2476. https://doi.org/10.1016/j.xphs.2016.01.010.

Thomas, N., Holm, R., Garmer, M., Karlsson, J.J., Mullertz, A., Rades, T., 2013. Supersaturated self-nanoemulsifying drug delivery systems (Super-SNEDDS) enhance the bioavailability of the poorly water-soluble drug simvastatin in dogs. AAPS. J. 15, 219–227. https://doi.org/10.1208/s12248-012-9433-7.

Thomas, N., Richter, K., Pedersen, T.B., Holm, R., Mullertz, A., Rades, T., 2014. *In vitro* lipolysis data does not adequately predict the *in vivo* performance of lipid-based drug delivery systems containing fenofibrate. AAPS. J. 16, 539–549. https://doi.org/10.1208/s12248-014-9589-4.

Williams, H.D., Anby, M.U., Sassene, P., Kleberg, K., Bakala-N'Goma, J.C., Calderone, M., Jannin, V., Igonin, A., Partheil, A., Marchaud, D., Jule, E., Vertommen, J., Maio, M., Blundell, R., Benameur, H., Carriere, F., Mullertz, A., Pouton, C.W., Porter, C.J., 2012a. Toward the establishment of standardized *in vitro* tests for lipid-based formulations. 2. The effect of bile salt concentration and drug loading on the performance of type I, II, IIIA, IIIB, and IV formulations during *in vitro* digestion. Mol. Pharm. 9, 3286–3300. https://doi.org/10.1021/mp300331z.

Williams, H.D., Sassene, P., Kleberg, K., Bakala-N'Goma, J.C., Calderone, M., Jannin, V., Igonin, A., Partheil, A., Marchaud, D., Jule, E., Vertommen, J., Maio, M., Blundell, R., Benameur, H., Carriere, F., Mullertz, A., Porter, C.J., Pouton, C.W., 2012b. Toward the establishment of standardized *in vitro* tests for lipid-based formulations, part 1: method parameterization and comparison of *in vitro* digestion profiles across a range of representative formulations. J. Pharm. Sci. 101, 3360–3380. https://doi.org/10.1002/jps.23205.

Wu, H.-S., Tsai, M.-J., 2004. Kinetics of tributyrin hydrolysis by lipase. Enzyme Microb. Technol. 35, 488–493. https://doi.org/10.1016/j.enzmictec.2004.08.002.

Zangenberg, N.H., Müllertz, A., Kristensen, H.G., Hovgaard, L., 2001. A dynamic *in vitro* lipolysis model I. Controlling the rate of lipolysis by continuous addition of calcium. Europ. J. Pharmaceut. Sci. 14, 115–122. https://doi.org/10.1016/S0928-0987(01)00169-5.